Published in final edited form as:
J Control Release. 2013 November 10; 171(3): 296–307. doi:10.1016/j.jconrel.2013.06.019.

Design and Evaluation of New pH-Sensitive Amphiphilic Cationic Lipids for siRNA Delivery

Anthony S. Malamas[†], **Maneesh Gujrati**[†], **China M. Kummitha**[†], **Rongzuo Xu**[†], and **Zheng-Rong Lu**[†,*]

[†]Department of Biomedical Engineering, Case Western Reserve University, Cleveland, Ohio 44106, USA

Abstract

Synthetic small interfering RNA (siRNA) has become the basis of a new generation of gene-silencing cancer therapeutics. However, successful implementation of this novel therapy relies on the ability to effectively deliver siRNA into target cells and to prevent degradation of siRNA in lysosomes after endocytosis. In this study, our goal was to design and optimize new amphiphilic cationic lipid carriers that exhibit selective pH-sensitive endosomal membrane disruptive capabilities to allow for the efficient release of their siRNA payload into the cytosol. The pH sensitive siRNA carriers consist of three domains (cationic head, hydrophobic tail, amino acid-based linker). A library of eight lipid carriers were synthesized using solid phase chemistry, and then studied to determine the role of (1) the number of protonable amines and overall pK_a of the cationic head group, (2) the degree of unsaturation of the hydrophobic tail, and (3) the presence of histidine residues in the amino acid linker for transfection and silencing efficacy. *In vitro* screening evaluation of the new carriers demonstrated at least 80% knockdown of a GFP reporter in CHO cells after 72 hours. The carriers ECO and ECLn performed the best in a luciferase knockdown study in HT29 human colon cancer cells, which were found to be more difficult to transfect. They significantly reduced expression of this reporter to 22.7±3.31% and 23.5±5.11% after 72 hours post-transfection, better than Lipofectamine RNAiMax. Both ECO and ECLn carriers caused minimal cytotoxicity, preserving relative cell viabilities at 87.3±2.72% and 88.9±6.84%, respectively. A series of hemolysis assays at various pHs revealed that increasing the number of amines in the protonable head group, and removing the histidine residue from the linker, both resulted in improved membrane disruptive activity at the endosomal pH of 6.5. Meanwhile, the cellular uptake into HT29 cancer cells was improved, not only by increasing the amines of the head group, but also by increasing the degree of unsaturation in the lipid tails. Due to flexibility of the synthetic procedure, the delivery system could be modified further for different applications. The success of ECO and ECLn for *in-vitro* siRNA delivery potentially makes them promising candidates for future *in-vivo* studies

[*]To whom correspondence should be addressed: Dr. Zheng-Rong Lu, M. Frank and Margaret Domiter Rudy Professor, Wickenden 427, Mail Stop 7207, 10900 Euclid Avenue, Cleveland, OH 44106, Phone: 216-368-0187, Fax: 216-368-4969, zxl125@case.edu.

Keywords

siRNA delivery; pH-sensitive amphiphilicity; endosomal escape; cationic lipid

1. Introduction

RNA interference (RNAi) is a natural antisense mechanism that cells possess to regulate the expression of genes at the mRNA level. This process relies on the ability of short fragments (19-23 nucleotides in length) of double stranded small interfering RNA (siRNA) to recognize and guide complementary mRNA transcripts into the RNA-induced silencing complex (RISC). Once translocated into RISC complexes, the mRNA transcripts are cleaved and ultimately degraded inside the cell, rendering them ineffective for translation into proteins. Meanwhile, the siRNAs are preserved and constantly recycled for further silencing events [1-4]. The ability to synthetically design siRNAs against particular mRNA sequences has triggered numerous clinical and pre-clinical studies to tailor RNAi induced silencing against a variety of disease-related genetic transcripts [5].

Delivery of siRNA with nanoparticles is desirable in order to overcome their susceptibility to serum nucleases and their ability to stimulate the innate immune system upon intravenous injection [6]. The use of nanoparticles can also prevent the possibility of off-target side effects. Nanoparticles are also required for successful siRNA therapies because they can facilitate intracellular release following uptake by tumor cells [7]. Endocytosis has been identified as a dominant cellular uptake mechanism, whereby foreign material delivered to cells will be sequestered into endosomal compartments and ultimately degraded after fusion with lysosomes [8]. As a result, siRNA therapy faces an additional delivery barrier because access to the RISC complexes in the cytoplasm is necessary for effective treatment [9]. Viral vectors have evolved for millions of years to become efficient carriers at introducing their genetic material into host cells. As a result, adenoviruses and retroviruses are currently explored as possible gene therapy vectors, but the success they have shown *in vivo* is masked by their potential to severely trigger the immune response. Compared to viral vectors, non-viral or synthetic vectors have many advantages, such as low immunogenicity, low production cost, and ease of modification, thus making them very attractive for siRNA delivery platforms [10]. However, much research is still required in order to improve upon the low transfection efficiencies of most current non-viral vectors [7].

Cationic lipid constructs are widely used as alternatives to viral nanoparticles. They form nanoparticles through the electrostatic interaction with the negatively-charged siRNA. Such nanoparticles, or lipoplexes, can be designed to exhibit similar characteristics and behaviors to those observed with viral vectors by utilizing pH sensitive moieties that facilitate endosomal escape [10]. This is typically accomplished by incorporating an amine-rich head group with an overall slightly acidic pK_a into the cationic lipid structure [11]. Once they become protonated in the acidic endosomal-lysosomal compartments, cationic lipoplexes are able to participate in membrane fusion and degradation events by inducing an electrostatic flip-flop reorganization of anionic phospholipids in the membrane bilayer [12-14]. This extensive transfer of lipids neutralizes the charge interactions that govern particle formation,

causing the inevitable dissociation of siRNA from the lipoplexes, followed by and subsequent release into the cytoplasm [15,16].

Recently, we have developed a series of novel polymerizable, pH-sensitive, amphiphilic lipid carriers for nucleic acid delivery. One of these carriers, EHCO, has undergone extensive testing in glioblastoma cell lines as a transfection agent for both plasmid DNA and siRNA. EHCO exhibited significant cell membrane disruption capabilities at the endosomal-lysosomal pH, while effectively preserving cell viability [17]. In addition, intravenous administration of targeted EHCO nanoparticles encapsulating anti-HIF-1α siRNA has demonstrated significant inhibition of tumor growth of a flank U87 tumor model [18]. The goal of this study was to introduce a variety of chemical modifications into the core structure of EHCO and then investigate how they will affect the physiochemical properties and performance of the lipid carrier as an siRNA transfection agent. To accomplish this, we have built a new library of pH-sensitive amphiphilic cationic lipid carriers and have evaluated their transfection capacity.

EHCO is a cationic lipid that is comprised of three primary domains: a protonable amine-based ethylenediamine head group, a hydrophobic group containing two mono-unsaturated oleic acid tails, and a histidine-cysteine amino acid based linker (Figure 1) [17,18]. Including EHCO, eight total carriers were synthesized to create the library of transfection agents. Two different chemical scaffolds were incorporated into each of the three domains of the delivery system to investigate (1) the effect of the number of amines of the head group, (2) the degree of unsaturation of the hydrophobic tail domain, and (3) the role of the protonatable histidine residue of the linker group on RNAi-mediated silencing efficacy (reference Figure 1). Nanoparticles of various N/P formulations were characterized and screened by a series of *in vitro* assays evaluating pH-sensitive membrane disruption, cellular uptake, cytotoxicity, and transfection efficiency to determine the optimal carrier and formulation for both a cancerous HT29 colon carcinoma and non-cancerous CHO (Chinese Hamster Ovary) cell line.

2. Materials and Methods

Materials

2-Chlorotrityl chloride resin, Fmoc-His(Trt)-OH, Fmoc-Cys(Trt)-OH, and benzotriazol-1-yl-oxytripyrrolidinophosphonium hexafluorophosphate (PyBOP) were purchased from EMD Biosciences (San Diego, CA). Ethylenediamine (EDA), spermine, piperidine, trifluoroacetic acid (TFA), 1,2-ethanedithiol (EDT), triisobutylsilane (TIBS), N,N′-diisopropylethylamine (DIPEA), oleic acid, linoleic acid, methyl acrylate, di-tert-butyl dicarbonate (Boc_2O), hydrazine, and TCEP (*tris*(2-carboxyethyl)phosphine) were purchased from Sigma-Aldrich (St. Louis, MO). Hydroxybenzotriazole (HOBt) was purchased from Peptides International (Louisville, KY). 2-Acetyldimedone (Dde-OH) was purchased from Chem-Impex International (Wood Dale, IN). ISOLUTE columns and accessories for all solid-phase synthesis reactions were purchased from Biotage (Charlotte, NC). All reactions were carried out under an atmosphere of dried nitrogen.

Anti-luciferase siRNA (sense sequence: 5′-CUUACGCUGAGUACUUCGAdTdT-3′, anti-sense sequence 5′-UCGAAGUACUCAGCGUAAGdTdT-3′) and anti-GFP siRNA (sense sequence: 5′-GCAAGCUGACCCUGAAGUUCAU-3′, antisense sequence: 5′-GAACUUCAGGGUCAGCUUGCCG-3′) were purchased from Dharmacon (Lafayette, CO). AlexaFluor488 labeled anti-luciferase siRNA was purchased from Qiagen (Valencia, CA).

Chinese Hamster Ovary cells stably expressing a green fluorescent reporter protein (CHO-d1EGFP) were provided by Dr. Charles Roth of Rutgers University. These cells were cultured in F-12K medium supplemented with 10% FBS (ATCC: Manassas, VA) under constant selective pressure by 500μg/mL geneticin (Invitrogen: Carlsbad, CA). HT29 human colon carcinoma cells were purchased from ATCC and stably transfected with a luciferase reporter enzyme. These cells were cultured in McCoy's 5A growth medium (Invitrogen) supplemented with 10% FBS, 100μg/mL streptomycin, and 100 units/mL penicillin.

Preparation of the lipid carriers

The multifunctional lipid carriers were synthesized by solid phase techniques in an ISOLUTE column reservoir. The preparation of all carriers followed a common synthetic procedure as outlined in Figure 2. The carriers with a spermine head group, SCHO and SHCLn, required masking of the two secondary amines of the spermine moiety at the initial stages of the synthesis to prevent unwanted side reactions. Standard peptide synthesis protocols were applied, using the ninhydrin test for detection of free primary amines to monitor reaction completion.

Representative preparation of SHCO (Figure 2)—2-Chlorotrityl resin **1** (500 mg, 1.58 mmol/g) was extensively washed with anhydrous DCM and allowed to swell for 2 hours. Then, the resin was washed 2x with DMF, mixed with spermine (1.6 g; 10x molar excess) in DMF (10 mL) and DIPEA (0.3 mL) under a dry nitrogen atmosphere and reacted for 2 hours. The resin was washed 3x with DMF and 3x with DCM to produce amine **2**. The chlorine residues on the resin that did not react with spermine were substituted by a methoxy group upon treatment with a mixture of MeOH/DIPEA/DCM (17/2/1 v/v/v) after a 30 min treatment. The resin was washed with DMF/DCM, mixed with Dde-OH (2.16 g) in DMF (10 mL) and DIPEA (0.3 mL) under an inert nitrogen atmosphere and reacted for 12 hours. Then, the resin was washed with DMF/DCM to afford diketone **3**. Boc_2O (17.24 g) was dissolved in DMF (10 mL) and DIPEA (0.6 mL) and the mixture was added to the resin under a nitrogen atmosphere and reacted for 6 hours. The resin was then washed with DMF/DCM to produce intermediate **4**. Three consecutive treatments of **4** with a solution of hydrazine (10 mL of 2% (v/v) in DMF) in 15 min interval periods, followed by a DMF/DCM wash, afforded intermediate **5**. Next, the resin was transferred into a round bottom flask with anhydrous DMF (10 mL). A large excess of methyl acrylate (50 mL) was added and allowed to react for 5 days at 50°C under an inert nitrogen atmosphere. Upon completion of the reaction, the resin was transferred back into an ISOLUTE column and washed with DMF/DCM to produce diester **6**. Next, the resin was transferred into another round bottom flask containing anhydrous DMF (10 mL) and ethylenediamine (50 mL) under an inert nitrogen atmosphere and reacted for 5 days at 50°C. Subsequently, the resin was

transferred back into a column and washed with DMF/DCM to yield bis-amine **7**. Fmoc-His(Trt)-OH amino acid (2 g) was added onto the resin with PyBop (1.6 g), HOBt (427 mg), and DIPEA (1.1 mL) in DMF (10 mL) under an inert nitrogen atmosphere and reacted for 4 hours. The resin was then treated with piperidine (20% (v/v) in DMF) three consecutive times with 20 min interval periods, followed by a DMF/DCM wash to afford intermediate **8**. At this stage, we repeated the same coupling procedure, as described above, by substituting Fmoc-Cys(Trt)-OH in place of Fmoc-His(Trt)-OH to generate intermediate **9**. The lipid tail was incorporated onto intermediate **9** by applying the same coupling procedure as above, but instead using oleic acid (1 mL) to produce intermediate **10**. The desired lipid carrier SHCO (**11**) was released from the resin upon treatment with a mixture of TFA/H_2O/EDT/TIBS (4 mL; 94/2.5/2.5/1 v/v/v) under an inert nitrogen atmosphere after 3 hours. The lipid carrier **11** was then precipitated by adding TFA into cold diethyl ether at a TFA:diethyl ether 1:40 volume ratio. The precipitated product was filtered and dissolved in a 50/50 mixture of water and acetonitrile and then purified using a reverse phase preparative HPLC gradient method (0 min: 10% ACN, 90% H_2O / 110 min: 100% ACN). An 1100 series Agilent HPLC system was used, equipped with a ZORBAX PrepHT C-18 column. Prior to each run on the HPLC, the lipid carrier was mixed with a 5x molar excess of a 1M TCEP solution to break any possible disulfide bonds that may have formed between the cysteine residues. The SHCO final product was characterized by using MALDI-TOF mass spectrometry (Bruker) and stored under nitrogen gas at -20°C to prevent oxidation of free thiols.

The SHCLn lipid carrier was prepared and purified similarly to SHCO, with the exception that linoleic acid (1mL) was used in place of oleic acid. The ethylenediamine-based carriers were also prepared according to the SHCO synthetic procedure, with the elimination of the initial primary amine protection (Dde-OH) and de-protection (hydrazine) steps, which were required in the spermine-based carriers in order to protect (Boc_2O) the secondary amines of the spermine moiety.

Particle formulation and characterization

The cationic lipid carriers are dissolved in ethanol at a stock concentration of 2.5 mM, while all siRNA is reconstituted in nuclease-free water at a 0.25 μg/μL (18.8 μM) concentration. Nanoparticles are formulated by mixing the carriers with siRNA for a period of 30 minutes in RNase-free phosphate buffer saline (PBS) at pre-specified N/P ratios (N = number of protonable amines in lipid, P = number of phosphate groups in the siRNA). In preparing the lipoplexes, proper dilutions were made such that the volume ratio of ethanol:water was kept constant at 1:20. Minimizing the amount of ethanol is important because it is effective in dissolving lipids, thus inhibiting particle formation. The diameters (as determined by dynamic light scattering) and zeta potentials of all nanoparticles were analyzed using a Malvern Zetasizer instrument at pH=7.4. siRNA encapsulation efficiency was calculated using a RiboGreen fluorescence-based assay from Invitrogen, designed specifically for detection of free RNA at emission and excitation wavelengths of 480 and 520 nm, respectively. Nanoparticles were created with all carriers in the library so that final siRNA concentrations were 1.6 μg/mL. A linear standard curve was utilized to calculate the encapsulation efficiencies from signal intensities measured by a SpectraMax microplate reader (Molecular Devices).

Intracellular gene silencing efficiency

The RNAi induced silencing capabilities of the each carrier was investigated in both a CHO-GFP non-cancerous cell line and an HT29-Luc (luciferase) human colon cancer cell line. Approximately 50,000 CHO-GFP cells were seeded into 6 well plates. When 25% confluency was achieved, the growth media was replaced with fresh serum-free transfection media containing siRNA nanoparticles, at a dose of 100 nM siRNA. Negative controls included cells that were either treated with naked anti-GFP siRNA or with plain serum-free media. N/P ratios of 4, 6, 8, 10, 12, and 14 were tested for each carrier to determine the optimal nanoparticle formulation. In order to compare the silencing capabilities of the agents designed in our library with commercially available alternatives, Lipofectamine RNAiMax particles were formulated and transfected according to the manufacturer specifications, and did not undergo changes in N/P ratios. After 4 hours, the media was removed and replaced with fresh complete growth media, and cells were allowed to grow for another 24, 48, or 72 hours post-transfection. At each of these time points, the CHO-GFP cells were rinsed twice with PBS, trypsinized, and fixed with 2% paraformaldehyde. Flow cytometry using a BD Biosciences FACSCalibur machine enabled us to determine the GFP expression in every sample. Cell-Quest software was used to analyze the results and obtain mean fluorescence intensity (MFI) values. GFP expression for each replicate was calculated relative to the control samples that did not receive any siRNA treatment.

Gene silencing efficiency was investigated in the HT29-Luc cell line by analyzing the expression of a luciferase reporter after anti-Luc siRNA therapy. To perform this study, cancer cells were seeded in 12 well plates at a density of 20,000 cells per well. Transfections were conducted in fresh serum-free media with 100 nM of siRNA when the cells were 25% confluent. The cells continued to grow in normal growth media for an additional 48 and 72 hours, at which point they were rinsed twice with PBS and lysed for protein collection. The lysis buffer was a component of a Promega Luciferase Assay kit designed for measuring luciferase expression in the cell lysate. Equally important, the lysis buffer was compatible with the BCA protein assay so that we were able to normalize the luciferase expression in our samples with total protein content. For this silencing study, all synthesized carriers were evaluated at N/P ratios of 8, 10, 12, 14, 16, 18, and 20 to determine the best transfection formulation. Relative luciferase expression was determined for each trial using a SpectraMax luminometer upon the addition of a light-inducing luciferin substrate to the collected protein.

Cytotoxicity

Cytotoxicity of the carriers was investigated using an MTT colorimetric assay measuring cellular metabolic activity (Invitrogen). The transfection procedure was identical to that presented for the reporter knockdown studies above, except for the fact that 96 well plates were utilized instead, and seeded with 10,000 cells per well. After transfection, the cells were allowed to grow for an additional 48 hours. At that point, they were incubated with MTT for 4 hours, followed by an additional 4 hour incubation with an SDS-HCl solution to dissolve any insoluble formazan crystals formed by the reduction of MTT by NAD(P)H-dependent enzymes in the cells. The absorbance of each sample was measured at 570 nm using a SpectraMax microplate reader. Cellular viability was calculated by averaging the

signal intensities over three replicates and then normalizing the results relative to the negative control data.

Cellular uptake via flow cytometry

Flow cytometry was used to investigate the cellular uptake of our delivery system in HT29 colon carcinoma cells. All carriers in the library were formulated into nanoparticles by condensing AlexaFluor-488 labeled siRNA at the optimal N/P ratio determined by the above luciferase knockdown studies. Approximately 50,000 cancer cells were seeded in 6-well plates and allowed to grow until 30-50% confluence was reached. The cancer cells were transfected with a 100 nM siRNA dose in serum-free media. After 4 hours, the transfection media was aspirated and the cells were washed twice with PBS. The cells were then trypsinized, collected, and fixed with 2% paraformaldehyde in PBS, prior to flow cytometric analysis.

Evaluation of pH-sensitive membrane disruption

Hemolytic activity of each carrier was determined to verify the pH-sensitive membrane disruption capabilities of each carrier in the delivery system. Red blood cells (RBCs) extracted from rats were purchased from Innovative Research Inc (Novi, MI) and diluted 1:50 in PBS solutions of pH =5.4, 6.5, or 7.4. A total of 100 μL of nanoparticles were created at N/P ratios of 5, 10, 15 and then incubated with 100 μL of diluted RBCs at 37°C for 2 hours. Nanoparticles were formulated so that the final amine concentration for all the samples, after mixing with the RBCs, was 150μM. Multiple pHs were tested to predict if the nanoparticles could disrupt membranes of the endosomal-lysosomal compartments (pH=5-6), without affecting the integrity of the outer cell membrane prior to endocytosis (pH=7.4). The absorbance of each test sample was measured on a SpectraMax spectrophotometer at a wavelength of 540nm in order to determine the amount of hemoglobin released from the RBCs, due to membrane destabilization, relative to that achieved by a positive control treatment of 1% (v/v) Triton-X100 surfactant during the 2 hour incubation period.

Intracellular release of siRNA

Live-cell confocal imaging was utilized to image the intracellular release and dispersion of siRNA following transfection with the lipid carrier that performed best during the reporter knockdown studies. Approximately 50,000 HT29-Luc cells were seeded onto glass-bottom dishes (MatTek – Ashland, MA). Once 40% confluency was established, the cells were stained with 75 nM LysoTracker Red DND-99 (Invitrogen) for 30 minutes in normal growth medium. Afterwards, the cells were transfected with 100 nM AlexaFluor488-labeled anti-Luc siRNA in fresh serum-free media using the designed cationic lipid agent that performed the best in the above reporter knockdown experiments. Imaging commenced 5 minutes post-transfection using an Olympus FV1000 confocal microscope, and continued periodically over the first two hours. Throughout the course of the study, all cells were kept alive on the microscope in a humidified weather station under normal gas conditions (5% CO_2). Another image was acquired after 24 hours following re-administration of the LysoTracker stain.

Statistical Analysis

Statistical analyses were performed using ANOVA and two-tailed Student's t-tests with a 95% confidence interval. Probability values of $p<0.05$ were considered significant.

3. Results

Synthesis of cationic lipid library

The structures and names of all eight cationic lipids in the designed library are shown in Figure 1. Each transfection agent represents a different combination of 2 protonable cationic head groups (ethylenediamine or spermine), 2 fatty acid tails (mono- or di-alkene unsaturated oleic and linoleic acid), and 2 linker domains (cysteine or histidine-cysteine). Peptide synthesis protocols were employed to create each carrier by solid phase chemistry, using the representative synthetic procedure for the preparation of the spermine-based carrier SHCO shown in Figure 2.

Carriers with an ethylenediamine (EDA) head group required fewer synthetic steps than their spermine-based analogues. After attaching the EDA head group onto 2-chlorotrityl resin, the reaction directly proceeded to the Michael addition of methyl acrylate to the primary amine. In contrast, preparation of the spermine carriers required two additional synthetic steps to mask the secondary amines of the spermine moiety and avoid unwanted side reactions. All final carriers were purified by preparative HPLC and verified by mass spectrometry. The calculated (m/z) and measured ($[M + H]^+$) molecular weights of each cationic lipid are summarized in Table 1. No evidence of byproducts was observed in any of the mass spectra.

Nanoparticle characterization and siRNA encapsulation

The complexation of cationic lipids with siRNA was investigated utilizing dynamic light scattering (DLS) and a RiboGreen fluorescence-based assay that can detect free, non-encapsulated RNA. Nanoparticle formation was observed when both the lipids and siRNA were mixed together at N/P ratios above 1.0, as determined by the RiboGreen assay (data not shown). However, few particles were formulated at this N/P ratio as evidenced by the fact that more starting materials were required to obtain a DLS reading.

Size, polydispersity, and zeta-potential data for each carrier at five different N/P ratios are shown in Tables 2-4. It was observed that particle diameter and polydispersity decreased as the N/P ratio was increased for each of the transfection agents, and no noticeable trend was observed between carriers with different head and/or lipid tail groups. Lipoplexes were generally greater than 400 nm in diameter at N/P=2, and then ranged between 42-75 nm at N/P=15. In addition, the zeta-potentials all appeared to increase with the N/P ratio as well. However, nanoparticles with spermine-based head groups exhibited a significantly quicker change in zeta-potential. The charges of these particles remained nearly constant between 23-28 mV at N/P=5 and above. However, those with EDA head groups exhibited a more gradual change in zeta-potential, and were still negative in charge at N/P=5. ECO and ECLn nanoparticles essentially reached their maximum positive charge density at N/P=8, unlike those made from EHCO and EHCLn, which did not attain their greatest electrostatic charge

density until N/P=15. In addition to their greater charge at N/P=8, ECO and ECLn lipoplexes were observed to be much smaller in size than their EHCO and EHCLn counterparts. siRNA encapsulation efficiency was nearly 100% for all spermine-base carriers at N/P formulations as low as 2; however 90% encapsulation for all EDA-based agents was not achieved until the N/P ratio was increased to 10 and above (Figure 3). This suggests that the spermine head groups, with two additional amines compared to their EDA counterparts, are more efficient at condensing siRNA into nanoparticles.

RNAi-mediated silencing of reporter proteins in CHO-GFP and HT29-Luc cells

Transfections were conducted in both a non-cancerous (CHO) and cancerous (HT29) cell lines in order to determine the silencing efficiency of each carrier upon delivery of siRNA against GFP and luciferase reporter proteins. It was found that RNAi-mediated knockdown was more effective as the N/P ratios were increased. Nanoparticle characterizations showed that increasing N/P made the lipoplexes more positively-charged and reduced their diameters, both of which are factors that can significantly improve cell uptake efficiency.

Figure 4 shows that only ECO and ECLn achieved greater than 20% knockdown in CHO-GFP cells at 24 and 48 hours post-transfection at N/P=4, reducing the relative reporter expression to 61.0±5.05% and 62.9±3.30%, respectively at the 48 hour time point. The zeta-potential data presented in Table 4 suggest that the lipoplexes they form at this N/P ratio are negative, potentially inducing electrostatic repulsion with the cell membrane during passive uptake. Transfection efficiencies were best at N/P=12 for all agents tested. Five out of the eight carriers were able to mediate at least 80% knockdown of the GFP reporter protein from 24-72 hours post-transfection. In fact, 6 of the 8 carriers out-performed the commercial agent Lipofectamine-RNAiMax after 72 hours by achieving longer-lasting silencing effects. Cytotoxicity at N/P=12 was minimal for all of the transfection agents, due to the fact that the lowest relative cell viability, as determined from an MTT assay, was 83.3±4.22% by the SHCLn lipid carrier. N/P ratios above 12 caused much greater levels of cytotoxicity, decreasing cell viability to approximately 40-50% for all carriers in the synthesized library.

The transfection efficiencies of the carriers were further determined in an HT29 human colon carcinoma cell line stably expressing a luciferase reporter. The silencing effects were apparent in the HT29 cells only after 48 hours post-transfection, as opposed to after 24 hours in the above CHO-GFP study (data not shown). However, like before, long-term silencing was still observed at the 72 hour time points. Figure 5 shows that greater N/P ratios were required to achieve significant knockdown effects, compared to those used for the CHO-GFP transfections. Carriers that achieved between 35-50% knockdown of the GFP reporter in CHO cells at the N/P=8 formulation, could only induce between 10-25% knockdown of the luciferase reporter in the HT29 cell line. When the N/P ratio was increased to 12, ECO and ECLn were found to perform significantly better than the other transfection agents. Luciferase expression was reduced to 33.5±3.82% and 45.8±1.88% by ECO and ECLn, respectively, after 72 hours. None of the other carriers reduced luciferase expression below 57.1±1.76%. These results were inferior to those obtained from the CHO-GFP transfections, and as a result, the N/P ratio was increased to 18 to further improve the silencing capability of each carrier. At this formulation, ECO and ECLn were able to reduce luciferase

expression to 22.7±3.31% and 23.5±5.11% of their pretreatment levels after 72 hours, which was superior to that achieved by Lipofectamine (29.4±2.29%). The rest of the carriers silenced reporter expression to between 34.0±4.76% and 53.7±5.75% relative to the negative control non-treated samples. Formulations at higher N/P ratios induced greater levels of cell death, with cell viabilities falling from 87.3±2.72% and 88.9±6.84% at N/P=18 to 51.5±5.87% and 53.7±6.92% at N/P=20 for the ECO and ECLn transfection agents, respectively.

Determination of hemolytic activity

In an attempt to understand why ECO and ECLn were the best carriers from the library, meeting our target of at least 75% knockdown efficiency with 80% cell viability, we first analyzed the membrane disruptive capabilities of each agent using a hemolysis assay. Figure 6 shows that all carriers exhibited significant pH-sensitive hemolytic activity, and that increasing the N/P ratios generally improved their membrane disruptive properties. It was also observed that increasing the N/P ratio from 10 to 15 did not affect the hemolytic activity at pH=5.4, but rather significantly improved RBC destabilization at pH=6.5, which is known to be the pH of the environment inside endosomal compartments. Therefore, it is possible that increasing the N/P ratio results in better RNAi-mediated reduction of HT29 luciferase expression by improving endosomal escape and allowing the delivery siRNA to evade the degradative lysosomal environment. Despite the fact that both ECO and ECLn possessed the greatest silencing efficiencies, they were not the most robust at inducing membrane destabilization events. Instead, the SCO and SCLn carriers exhibited the greatest hemolytic activity relative to Triton X-100 at all N/P ratios and pHs tested. Nonetheless, the degree of hemolytic activity ECO and ECLn expressed at pH=6.5 was also matched by SHCO and SHCLn, even though these cationic lipids were not as effective in transfecting the HT29 cancer cells.

Cellular Uptake

Flow cytometry was utilized to determine the cellular uptake of each carrier complexed with AlexaFluor488-labeled siRNA at N/P=18. The mean fluorescence intensity (MFI) values presented in Figure 7 were calculated from the acquired histograms and used to determine if cellular uptake was correlated to transfection efficiency in HT29 cancer cells. Similar to hemolytic results, ECO and ECLn did not possess the best uptake efficiencies despite their superior performance in the transfection studies. Their mean fluorescence intensities were 2571±90 and 3423±115, respectively, while those of SHCLn and SCLn were 4414±413 and 4066±185. The results also show that better cellular uptake was achieved when di-unsaturated linoleic acids were incorporated into the hydrophobic domains in place of mono-unsaturated oleic acid tails (reference the above ECO/ECLn MFIs as an example). In addition, spermine-based agents showed significantly higher uptake than their EDA counterparts (EHCO MFI = 1957±208 as opposed to SHCO MFI = 3580±244).

Intracellular siRNA release

Confocal microscopy was utilized to perform a time course study that analyzed the uptake and intracellular release kinetics of siRNA using the ECO delivery platform. Intracellular release and dispersion of siRNA is essential in RNA interference since the RNAi machinery

is found primarily in the cytosol. ECO-siRNA nanoparticles were prepared in the same manner that was implemented for the reporter knockdown studies, with the exception that the siRNA was now labeled with a fluorophore. Figure 8 reveals that the ECO lipoplexes facilitated the escape of its siRNA payload from the endocytic pathway within the first 90 minutes after transfection, avoiding lysosomal entrapment degradation. This was evident by the lack of co-localization between the Alexafluor488-labeled siRNA and the LysoTracker Red stain. siRNA dispersion was present in almost all cells 24 hours post-transfection. Such results are in congruence with the hemolytic activity data demonstrating the membrane disruptive property of ECO in low pH environments, which is required for siRNA escape from both endosomes and early lysosomes.

4. Discussion

The primary focus of this study was to design and optimize a new library of pH-sensitive amphiphilic cationic lipid carriers for RNAi therapy. The delivery system is comprised of three main components: (1) a protonable cationic head groups; (2) a lipophilic domain containing two fatty acid tails; and (3) an amino acid based linker, as illustrated in Figure 1. Each domain of the delivery system was modified with two different chemical groups in order to analyze how subtle structural changes are able to adjust and fine-tune the efficiency of RNAi-mediated gene silencing events in a CHO Chinese Hamster Ovary and an HT29 human colon carcinoma cell line. All carriers were constructed off a resin using standard solid phase peptide synthesis protocols so that the library could be easily expanded without changing the overall reaction scheme. The modifications introduced into the library all play a role in the pH sensitive membrane disruptive capabilities of the carriers, and as a result, provide insight on how the structures and physiochemical properties of the delivery system can enhance the cellular uptake and endosomal release mechanisms during siRNA therapy.

Ethylenediamine (EDA) and spermine are multivalent organic compounds that are extensively studied in antisense delivery systems [19-22]. They possess two and four amine groups, respectively, and thus carry a net positive charge at neutral pH. When incorporated into the head groups of our cationic lipid carrier, they are responsible for electrostatic condensation of siRNA to form inverted micelles in PBS buffer. The amines in the head groups also contribute to the essential pH-sensitive characteristic of our delivery system, which is important for improving endosomal escape and RNAi-mediated silencing efficiency. Greater protonation of the amine head groups can occur in the relatively acidic environment (pH=5-6) of the endosome and lysosome compartments after cellular uptake [10,11]. This enhances electrostatic interactions between the cationic carriers and the anionic phospholipids of endosomal/lysosomal membranes, promoting the bilayer destabilization and nanoparticle charge neutralization events required for efficient cytosolic release of their siRNA payload [16]. By affecting the number of amines, and thus overall pK_a, of the cationic carrier, the choice of head group (in this case EDA or spermine) can ultimately determine the degree to which such protonation can occur [11]. The pH-sensitive property of the delivery system is essential so that the nanoparticles do not affect the integrity of the outer cell membrane and cause cell death, but instead are able to selectively fuse with and destabilize the endosomal and lysosomal membranes.

Although the presence of cationic charges in the head group is important for endosomal membrane disruption, the chemical makeup of the hydrophobic tail groups is another factor that dictates how efficiently the necessary fusion events will occur. In particular, we were interested in analyzing the effects of varying the degree of unsaturation within the hydrophobic tail domain on the transfection capabilities. Gruner et al. have concluded that the fusion between two lipid membranes is mediated by a lamellar-to-hexagonal inverted phase transition. However, this phenomenon cannot occur without the use of conical shaped lipids, meaning that the effective cross-sectional area of the hydrophilic head groups is smaller than that of the hydrophobic tails [13,23,24]. DOPE is a widely utilized helper lipid incorporated into liposomal formulations because it possesses the desired conical shape to help mediate hexagonal phase transition and improve overall transfection efficiencies [25].

In general, the transfection efficiency of cationic lipid carriers has been shown to decrease with increasing alkyl chain length and saturation [26]. When saturated, shorter aliphatic chains (C_{12} and C_{14}) favor higher rates of inter-membrane lipid mixing and reportedly allow for better transfection efficiencies *in vitro*, as compared to *in vivo*, whereas the opposite is true for longer chains (C_{16} and C_{18}) [17,27]. Typically, saturated fatty acids greater than 14 carbons in length are not favorable for nucleic acid transfections due to their elevated phase transition temperature and overall less fluidity than those that are unsaturated [28]. However, it has been discovered that there exists a limit, at which point an increase in unsaturation and lipid fluidity is inversely correlated to transfection efficiency, primarily because some degree of rigidity is required for particle stability, as evidenced by the widespread use of cholesterol in lipid nanoparticle formulations [26,29].

The hydrophobic tail domain of our delivery system contains two oleic or linoleic acid (mono- and di-alkene unsaturated) 18 carbon fatty acids. The additional double bond in linoleic acid introduces an extra kink into the hydrocarbon backbone, giving the lipid a broader conical shape than oleic acid and increasing its fluidity. When incorporated into a nanoparticle structure, the extra degree of unsaturation elevates the propensity to form the hexagonal phase during an impending membrane fusion event of cellular uptake [30]. However, some ambiguity remains as to which aliphatic chain will perform better for transfections, especially when considering variations in the cellular trafficking mechanics of different cell lines. Studies have shown that cellular uptake and silencing efficiency with linoleic acid is lower than that of oleic acid, while others have found that even with lower uptake, RNAi induced knockdown was actually higher [30,31]. This suggests that the choice of fatty acid in the lipoplex design likely plays an important role in endosomal escape after cellular uptake, and thus needs to be optimized for our siRNA delivery platform.

The nature of the linker group bridging the protonable cationic head group and the hydrophobic tail domain has also been correlated with transfection efficiencies of various nucleic acid delivery systems [26]. One common feature between the two different linker domains employed in the design of our cationic lipid library was the presence of polymerizable cysteinyl residues. Since our lipid-siRNA nanoparticles are made in oxidative conditions, free thiols in close proximity to one another will react to form disulfide bonds that are primarily reducible by glutathione and the oxidative conditions found inside the cell [32]. This imparts a degree of stability unmatched by similar cationic lipid siRNA delivery

systems during the uptake process. The cysteinyl residues are also included into the construct because their thiol groups can also be functionalized to improve the pharmacodynamic performance of the delivery system *in vivo*. As previously described by Wang et al, a low molecular weight bi-functional polyethylene glycol (PEG) polymer, modified on one end with a cyclic RGD targeting moiety, can be conjugated to the free thiol group on our carriers via a maleimide linkage [18]. PEG is commonly used to improve the bioavailability and systemic circulation of many drug delivery platforms by preventing serum opsonization and subsequent clearance by the reticuloendothelial system (RES) [33]. Meanwhile, cRGD is also a common targeting moiety that binds to $\alpha_v\beta_3$ integrins over-expressed on the endothelial surface of tumor vasculature, and can thus eliminate off-target silencing effects once administered into the body [34].

In addition to the cysteine residues, histidine groups were also incorporated into the linker domains of some of the siRNA carriers. With a pK_a around 6, the imidazole ring of histidine is a weak base that has the ability to acquire a cationic charge when the pH of the environment drops below 6, as is the case inside the endosomal compartments after cellular uptake. In the unprotonated state, the imidazole has one donor and one acceptor site for hydrogen bonding, thus stabilizing the lipoplex structure following particle formation [11]. However, after protonation, this heterocycle now possesses two donor sites for hydrogen bonding that can induce disruption of the supramolecular network and increase the fusogenic characteristic of the formulation. As a result, histidine has been shown to fine-tune the pH sensitivity of many cationic lipid, polymeric, and dendrimer-based delivery systems, resulting in the significant improvement of RNAi-mediated silencing [11].

All lipid carriers in this study were screened over various N/P ratios in both CHO and HT29 cell lines in order to determine the optimal transfection agent and formulation. N/P ratios between 2 and 20 were utilized for the various *in vitro* assays performed in this study. The number of protonable amines is largely responsible for membrane destabilization and subsequent endosomal release. As a result, increasing the amines, without inducing cytotoxicity, significantly improves transfection efficiency. Therefore, since each carrier in the library possessed a different number of protonable amines, it was essential to compare their physiochemical properties at the same N/P ratios, or amine concentrations, rather than the same lipid concentrations. Otherwise, carriers such SCHO/SCHL (with 6 protonable amines) would perform better than ECO/ECLn (with 2 protonable amines) not because it is a more efficient delivery agent, but because the test samples would be overloaded with more amines.

In the non-cancerous CHO cell line, each carrier was able to achieve significant knockdown of a GFP reporter protein as the N/P ratio was increased above 4. Little to no silencing by almost all of the transfection agents was observed at this formulation, likely stemming from the fact that their negative zeta potentials cause an electrostatic repulsion with the negatively charged cellular membranes. Five out of the eight agents induced at least 80% knockdown at N/P=12, while the remaining 3, including the original carrier EHCO, exhibited silencing efficiencies that paralleled those of Lipofectamine RNAiMax 72 hours after transfection. The N/P=12 formulation was determined to be optimal for CHO cell transfection since it facilitated the greatest levels of GFP knockdown without significantly compromising

cellular viability, as determined by MTT assay. In addition, the lipid carriers exhibited superior long-term effectiveness over Lipofectamine, as evidenced by the lack of increase in GFP expression of transfected CHO cells at both 48 and 72 hours post-transfection.

Transfections with the HT29 colon cancer cells were not as robust compared to those conducted with the CHO line. The optimal N/P ratio was 18 when transfecting the HT29 cells, meaning that more carrier was required to facilitate the luciferase silencing. Nevertheless, none of the delivery agents were able to silence the reporter at the levels observed during the CHO-GFP study. The two best carriers were ECO and ECLn, which were able to achieve 77.5±3.3% and 76.5±5.1% knockdown 72 hours post-transfection. Both agents performed significantly better than the parent compound EHCO, with a transfection efficiency of only 46.4±5.8%. Although the reporter genes in each cell line were different, Lipofectamine was able to silence both reporters equally well under the same transfection conditions and formulations. This suggests that the variable efficacy of our pH-sensitive delivery system is largely cell-type dependent. RNAi therapy is greatly impacted by the ability of siRNA to be taken up by the cells during endocytosis, and then to subsequently escape the endosomal compartments before lysosomal degradation. Each phenomenon was investigated separately to understand and correlate how modifications in the cationic lipid delivery system affected the performance of each carrier in the HT29 transfection studies.

Hemolysis studies are commonly implemented in siRNA therapeutic research to assess the potential endosomolytic capabilities of new delivery systems at pH values that mimic endosomal trafficking [17,35-37]. By incubating the lipid-siRNA nanoparticles with rat erythrocytes at different pHs, and observing the release of hemoglobin into the surrounding medium, it can be determined whether the delivery system is able to promote endosomal membrane disruption required to release the nucleic acid into the cytoplasm, where it can then locate RISC complexes and mediate mRNA degradation. Figure 6 shows that all synthesized carriers exhibited significant improvement in membrane disruptive activity at pHs 6.5 and 5.4 (characteristic of early and late endosomes), than at pH=7.4 (extracellular) for N/P formulations between 5 and 15. In general, the hemolytic activity was not affected by the choice of fatty acid tail for the hydrophobic domain of the delivery system. However, increasing the number of amines in the head group improved hemolytic activity, as all spermine-based carriers performed better than their EDA-based analogues at pH=6.5 (i.e. SHCO/SHCLn was more efficient than EHCO/EHCLn, and SCO/SCLn was more efficient than ECO/ECLn). Lipid carriers with spermine in their head groups possess a greater number of positive charges after protonation in acidic environments. This can potentially improve their ability to electrostatically interact with anionic phospholipids in the red blood cell membrane and better promote bilayer destabilization.

However, the presence of additional protonable amines does not necessarily translate to better hemolytic activity. Although histidine possesses a protonable amine, lipid carriers containing this chemical moiety in their linker domain actually exhibited weaker membrane disruptive capabilities than their counterparts. At pH=6.5, EHCO and EHCLn both had lower hemolytic activity than ECO and ECLn, and the same discovery was made for SHCO/SHCLn and their SCO/SCLn counterparts. The incorporation of histidine into the delivery

system likely reduces the overall pK_a of the cationic lipids [11]. As a result, the pH-sensitivity of the carriers will increase, and thus potentially reduce the ability of each agent to protonate and electrostatically fuse with the RBC membrane bilayers at this level of acidity. This suggests that the ECO and ECLn based nanoparticles may better fuse with the membranes of early endosomes (pH=6.5) than the parent EHCO complexes, and therefore contribute to their superior silencing efficiencies observed in the reporter knockdown studies. Nevertheless, a steric effect may also play a significant role in the weaker membrane disruptive behavior observed upon introduction of the histidine residue. As discussed by Semple et al, geometrical shape of the transfection agent potentially plays a role in membrane fusion during RNAi mediated therapies. Cone-shaped cationic lipids have the ability to interact with anionic phospholipids in the endosomal membrane and form ion pairs that adopt non-bilayer structures with the ability to induce bilayer disruption in these compartments [38]. Histidine is an amino acid that contains an imidazole ring in its side chain. Including this chemical group into the linker for each hydrophobic tail can potentially increase the cross-sectional area of the hydrophilic portion of the lipid, favoring a more cylindrical shape that supports a bilayer structure. As evidenced by the fact that ECO, ECLn, SHCO, and SHCLn have similar hemolytic capabilities, it appears that the geometrical shape, the overall pK_a, and the number of protonable amines in the lipid construct all appear to represent competing factors that determine the ability of our delivery system to facilitate membrane disruption in various pH environments. Ideally, these properties should contribute to the endosomal escape and intracellular dispersion mechanisms of therapeutic siRNA.

Cellular uptake of AlexaFluor488-labeled siRNA (100nM) by HT29 colon cancer cells was measured by flow cytometry after a 4 hour incubation period with lipid nanoparticles formulated at N/P=18. It was demonstrated that cellular uptake mediated by the EHCO/EHCLn carriers was not as robust compared to that of SHCO/SCHLn, matching the same trend observed when using the ECO/ECLn and SCO/SCLn compounds. This finding suggests that the greater amine-rich head group is more favorable for passive uptake and delivery into cells, even though all siRNA-lipid nanoparticles possessed similar sizes (45-75nm in diameter) and zeta-potentials (25-30mV). Incorporating histidine into the linker domain, and thus two additional protonable amines, actually reduced nanoparticle uptake for EDA-based carriers, but did not have a significant impact when spermine was utilized. This can be attributed to why ECO and ECL each possessed better cellular uptake kinetics than the parent EHCO transfection agent. Nonetheless, unlike the hemolysis study, it was determined that the degree of unsaturation did in fact play a role in cellular uptake properties. The greater uptake of siRNA using transfection agents with the di-unsaturated linoleic acid fatty acid tails can possibly be attributed to increased lipid fluidity, as other studies have found that this anisotropic feature can enhance fusion, and not membrane destabilization, with bi-layered liposomal vesicles [30].

Despite the fact that ECO and ECLn were the optimal carriers for the luciferase knockdown study in the HT29 tumor cells, they exhibited neither the greatest membrane disruptive nor the highest cellular uptake capacity in the *in vitro* experiments. ECO, for example, did not perform as well as SCO/SCLn at any pH in the hemolytic study, nor did it match their levels

of cellular uptake. A similar observation can be made with SHCLn. Since ECO was still able to achieve better RNAi silencing effects of the luciferase reporter, it is possible that the intracellular trafficking mechanisms and pathways within the cell might not be the same for each carrier designed in the library, and is thus responsible for the lack of correlation in the trends observed from the endosomolytic/uptake data and the RNAi knockdown study. Similarly, it is also possible that the superior condensation properties of spermine-based carriers like SCO/SCLn, as evidenced by the encapsulation data, severely inhibited the rapid intracellular release of their siRNA payloads during endosomal membrane fusion. Progressively increasing the number of positive charges, or multi-valency, of the head group may result in too strong of an interaction with siRNA, such that it significantly hampers their ability to dissociate inside the cell [26].

The confocal images shown in Figure 8 reveal that ECO is able to facilitate efficient uptake and intracellular release of administered siRNA, as seen by the disperse AlexaFluor488 signal throughout the cell. The lack of co-localized signal with Lysotracker Red suggests that the nanoparticles are able to evade lysosomal degradation within 1 hour post-transfection. However, these images do not uncover the specific route that the lipid-siRNA nanoparticles take inside the cell before releasing its nucleic acid contents. Future intracellular tracking studies should include the use of antibody stains and inhibitors of specific proteins inside the cell involved with clathrin-mediated endocytosis in order to resolve where the particles are shuttled upon uptake, when they release their siRNA payload, and if they are exported outside the cell before having any therapeutic effect [39]. Caveolae-mediated endocytosis should also be studied considering that several nanomaterials reported to enter cells via this mechanism were also able to bypass lysosomal compartments [8]. Such experiments can ultimately reveal why certain lipid carriers in the library did not perform as well as some of their analogues. For example, SCO and SCLn were shown to exhibit around 40-50% of its maximum hemolytic activity at pH=7.4, meaning that they may have the ability to significantly fuse with the cell membrane in normal growth conditions, and not selectively within the more acidic endocytic and lysosomal compartments. However, since the MTT assay fails to show a significant degree of cytotoxicity from these carriers, it is possible that these carriers cannot induce the necessary hexagonal phase transition to destabilize the cell membrane and release its contents intracellularly. Cytoskeleton and other proteins, such as clathrin, that impart membrane stability likely prevent this from occurring and inhibit such lipoplexes from penetrating the cell [13].

The intracellular trafficking studies proposed above will also further validate the use of hemolysis as a surrogate for endosomal escape. Identifying RNAi transfection agents that possess poor hemolytic behavior at endosomal-lysosomal pH, and imaging the time dependent co-localization patterns between fluorescently labeled endosomes and siRNA can allow us to determine the extent to which ECO and ECLn enhance endosomal release and subsequent intracellular dispersion of their payload. However, it is also essential to test compounds that have equal hemolytic activities at pH 7.4 to eliminate the contribution of direct siRNA passage through the external cell membrane.

It is important to note that all transfections in this study were conducted in the absence of serum, which has been shown to reduce the transfection efficiency of cationic lipid-nucleic

acid complexes in cell culture experiments. Increasing the charge ratio is one strategy that can be used to overcome the inhibitory effects of serum [40,41]. Introducing PEG into the nanoparticle construct is another approach, which can effectively mask the complexes from serum proteins that bind and diminish the ability of the transfection agents to deliver their genetic payload [33].

Nevertheless, incorporating PEG into the complexes can also alleviate non-specific cell membrane interactions *in vivo* that may occur with our delivery system. Figure 6 shows that while the optimal ECO and ECLn lipid-based complexes possess significant hemolytic capabilities at N/P=15 within the endosomal-lysosomal pH ranges, these particles also exhibit membrane disruptive behavior at normal physiological pH of 7.4. This can be attributed to electrostatic interactions between negatively charged cell membranes and the inherent positive charges of both lipoplexes, as shown by the zeta-potential data presented in Table 4 above. Although their hemolytic efficiencies in relation to Triton X-100 are rather low, at 19% and 26% respectively, the ECO and ECLn complexes will have the ability to modestly interact with a variety of cell types as they pass through the body on their way to tumor tissues of interest, ultimately reducing the effectiveness of the therapy. In order to prevent the added PEG from interrupting the membrane fusion events necessary for intracellular dispersion of siRNA, acid-labile bonds, such as hydrazone linkages, can be utilized to facilitate the release of PEG as the particles are taken up and shuttled to the endosomal-lysosomal compartments [37].

In summary, we have shown structural dependent RNAi activity mediated by the amphiphilic cationic lipids. Increasing the number of protonatable amino groups in the head group enhanced complexation of the lipids with siRNA, but did not result in better gene silencing efficiency. The incorporation of histidine residues in the EDA based lipids increased pH-sensitive hemolysis by reducing hemolytic activity at higher pHs (6.5 and 7.4), and resulted in lower gene silencing efficiency as compared to the corresponding lipids without histidine residues. The unsaturation degree of the lipid tails did not affect the silencing efficiency of the lipids. The incorporation of cysteine residues was useful to enhance the stability of the particles, and important for the modification of surface properties of the nanoparticles.

5. Conclusion

A library of eight cationic amphiphilic carriers for siRNA delivery was designed with an optimized reaction scheme employing solid-phase peptide synthesis techniques. All transfection agents were structural modifications of the original EHCO carrier that was previously published. While the majority of the lipid carriers in the library performed extremely well in CHO cells, even better than the commercially available Lipofectamine RNAiMax, two carriers in particular (ECO and ECLn) achieved significantly greater luciferase silencing than the rest in an HT29 colon cancer cell line that was more difficult to transfect, including the parent compound EHCO. However, this study showed instances where ECO and ECLn did not possess superior endososmal release and cellular uptake properties compared to other transfection agents in the library, contrary to what was otherwise suggested by the RNAi-mediated silencing studies. These observations raise some

questions as to whether the intracellular trafficking mechanisms are different for each carrier and contribute to the variations observed in their transfection efficiencies. The pH-sensitive amphiphilic delivery system designed in this study is promising for future RNAi therapies, and can easily be fine-tuned further with other structural components due to the flexibility of the synthetic protocol.

References

1. Whitehead KA, Langer R, Anderson DG. Knocking down barriers: advances in siRNA delivery. Nat Rev Drug Discovery. 2009; 8:129–1138.
2. Miele E, Spinelli GP, Miele E, Di Fabrizio E, Ferretti E, Tomao S, Gulion A. Nanoparticle-based delivery of small interfering siRNA: challenges for cancer therapy. Int J Nanomedicine. 2012; 7:2637–2657.
3. Elbashir SM. Duplexes of 21-nucleotide RNAs mediate RNA interference in cultured mammalian cells. Nature. 2001; 411:494–498. [PubMed: 11373684]
4. Burnett JC, Rossi JJ. RNA-based therapeutics: current progress and future prospects. Chem Biol. 2012; 19:60–71. [PubMed: 22284355]
5. Davidson BL, McCray PB. Current prospects for RNA interference-based therapies. Nat Rev Genet. 2011; 12:329–340. [PubMed: 21499294]
6. Whitehead KA, Dahlman JE, Langer RS, Anderson DG. Silencing or stimulation? siRNA delivery and the immune system. Annu Rev Chem Biomol Eng. 2011; 2:77–96. [PubMed: 22432611]
7. Zhu L, Mahato RI. Lipid and polymeric carrier-mediated nucleic acid delivery. Expert Opin Drug Deliv. 2010; 7(10):1209–1226. [PubMed: 20836625]
8. Sahay G, Alakhova DY, Kabanov AV. Endocytosis of nanomedicines. J Controlled Release. 2010; 145:182–195.
9. Zabner J, Fasbender AJ, Moninger T, Poellinger KA, Welsh MJ. Cellular and Molecular barriers to gene-transfer by a cationic lipid. J Biol Chem. 1995; 270:18997–19007. [PubMed: 7642560]
10. Zhang XX, McIntosh TJ, Grinstaff MW. Functional lipids and lipoplexes for improved gene delivery. Biochimie. 2012; 94:42–58. [PubMed: 21621581]
11. Midoux P, Pichon C, Yaouanc J-J, Jaffrès P-A. Chemical vectors for gene delivery: a current review on polymers, peptides and lipids containing histidine or imidazole as nucleic acids carriers. Br J Pharmacol. 2009; 157:166–178. [PubMed: 19459843]
12. Hafex IM, Ansell S, Cullis PR. Tunable pH-sensitive liposomes composed of mixtures of cationic and anionic lipids. Biophys J. 2000; 79:1438–1446. [PubMed: 10969005]
13. Wrobel I, Collins D. Fusion of cationic liposomes with mammalian cells occurs after endocytosis. Biochim Biophys Acta. 1995; 1235(2):296–304. [PubMed: 7756338]
14. Gruner SM, Cullis PR, Hope MJ, Tilcock CPS. Lipid polymorphism: the molecular basis of nonbilayer phases. Ann Rev Biophys Biophys Chem. 1985; 14:211–238. [PubMed: 3890880]
15. Zelphati O, Szoka FC Jr. Mechanism of oligonucleotide release from cationic liposomes. PNAS. 1996; 93:11493–98. [PubMed: 8876163]
16. Xu Y, Szoka FC Jr. Mechanism of DNA release from cationic liposome/DNA complexes using in cell transfection. Biochemistry. 1996; 35:5616–5623. [PubMed: 8639519]
17. Wang X-L, Ramusovic S, Nguyen T, Lu Z-R. Novel polymerizable surfactants with pH-sensitive amphiphilic and cell membrane disruption for efficient siRNA delivery. Bioconjugate Chem. 2007; 18(6):2169–2177.
18. Wang X-L, Xu R, Wu X, Gillespie D, Jensen R, Lu Z-R. Targeted systemic delivery of a therapeutic siRNA with a multifunctional carrier controls tumor proliferation in mice. Mol Pharmaceutics. 2009; 6(3):738–746.
19. Blagbrough IS, Metwally AA, Ghonaim HM. Asymmetric N^4,N^9-diacyl spermines: SAR studies of nonviral lipopolyamine vectors for efficient siRNA delivery with silencing of EGFP reporter gene. Mol Pharmaceutics. 2012; 9:1853–1861.

20. Ahmed OAA, Pourzand C, Blagbrough IS. Varying the unsaturation in N^4,N^9-dioctadecanoyl spermines: nonviral lipopolyamine vectors for more efficient plasmid DNA formulation. Pharm Res. 2006; 23(1):31–40. [PubMed: 16382281]
21. Xu R, Lu Z-R. Design, synthesis and evaluation of spermine-based pH-sensitive amphiphilic gene delivery systems: Multifunctional non-viral gene carriers. Sci China Chem. 2011; 54:359–368.
22. Xu R, Wang X, Lu Z-R. Intracellular siRNA delivery with novel spermine based surfactants. Chin Sci Bull. 2012; 57:3979–3984.
23. Tseng YC, Mozumdar S, Huang L. Lipid-based systemic delivery of siRNA. Adv Drug Deliv Rev. 2009; 61(9):721–731. [PubMed: 19328215]
24. Hafez IM, Maurer N, Cullis PR. On the mechanism whereby cationic lipids promote intracellular delivery of polynucleic acids. Gene Ther. 2001; 8:1188–1196. [PubMed: 11509950]
25. Farhood H, Serbina N, Huang L. The role of dioleoyl phosphatidylethanolamine in cationic liposome mediated gene transfer. Biochim Biophys Acta. 1995; 1235:289–295. [PubMed: 7756337]
26. de Lima MCP, Neves S, Filipe A, Düzgüşnes N, Simões S. Cationic liposomes for gene delivery: from biophysics to biological applications. Curr Med Chem. 2003; 10:1221–1231. [PubMed: 12678796]
27. Zhi DF, Zhang SB, Wang B, Zhao YN, Yang BL, Yu SJ. Transfection efficiency of cationioc lipids with different hydrophobic domains in gene delivery. Bioconjugate Chem. 2010; 21:563–577.
28. Heyes JA, Niculescu-Duvaz D, Cooper RG, Springer CJ. Synthesis of novel cationic lipids: effect of structural modification on the efficiency of gene transfer. J Med Chem. 2002; 45:99–114. [PubMed: 11754582]
29. Balasubramanian RP, Bennet MJ, Aberle AM, Malone JG, Nantz MH, Malone RW. Structural and functional analysis of cationic transfection lipids: the hydrophobic domain. Gene Ther. 1996; 3:163–172. [PubMed: 8867864]
30. Le Gall T, Loizeau D, Picquet E, Carmony N, Yaouanc J-J, Burel-Deschamps L, Delépine P, Giamarchi P, Jaffrès PA, Lehn P, Montier T. A novel cationic lipophosphoramide with diunsaturated lipid chains: synthesis, physiochemical properties, and transfection activities. J Med Chem. 2010; 53:1496–1508. [PubMed: 20112994]
31. Heyes J, Palmer L, Bremner K, MacLachlan I. Cationic lipid saturation influences intracellular delivery of encapsulated nucleic acids. J Controlled Release. 2005; 107:276–287.
32. Wang X-L, Nguyen T, Gillespie D, Jansen R, Lu Z-R. A multifunctional and reversible polymerizable carrier for efficient siRNA delivery. Biomaterials. 2008; 29:15–22. [PubMed: 17923154]
33. Guo S, Huang L. Nanoparticles escaping RES and endosome: challenges for siRNA delivery for cancer therapy. J of Nanomaterials. 2011:1–12.
34. Ruoslahti E. RGD and other recognition sequences for integrins. Annu Rev Cell Dev Biol. 1996; 12:697–715. [PubMed: 8970741]
35. Henry SM, El-Sayed MEH, Pirie CM, Hoffman AS, Stayton PS. pH-responsive poly (styrene-alt-maleic anhydride) alkylamide copolymers for intracellular drug delivery. Biomacromolecules. 2006; 7(8):2407–2414. [PubMed: 16903689]
36. Convertine AJ, Benoit DSW, Duvall CL, Hoffman AS, Stayton PS. Development of a novel endosomolytic diblock copolymer for siRNA delivery. J Controlled Release. 2009; 133:221–229.
37. Lin Y-L, Jiang G, Birrell LK, El-Sayed MEH. Degradable, pH-sensitive, membrane-destabilizing, comb-like polymers for intracellular delivery of nucleic acids. Biomaterials. 2010; 31:7150–7166. [PubMed: 20579726]
38. Semple SC, Akinc A, Chen J, Sandhu AP, Mui BL, Cho CK, et al. Rational design of cationic lipids for siRNA delivery. Nat Biotechnol. 2010; 28(2):172–178. [PubMed: 20081866]
39. Rejman J, Bragonzi A, Conese M. Role of clathrin- and caveolae-mediated endocytosis in gene transfer mediated by lipo- and polyplexes. Mol Ther. 2005; 12(3):468–474. [PubMed: 15963763]
40. Yang J-P, Huang L. Time-dependent maturation of cationic liposome–DNA complex for serum resistance. Gene Therapy. 1998; 5:380–387. [PubMed: 9614558]

41. Nchinda G, Überla K, Zschörnig O. Characterization of cationic lipid DNA transfection complexes differing in susceptibility to serum inhibition. BMC Biotechnology. 2002; 2(12)

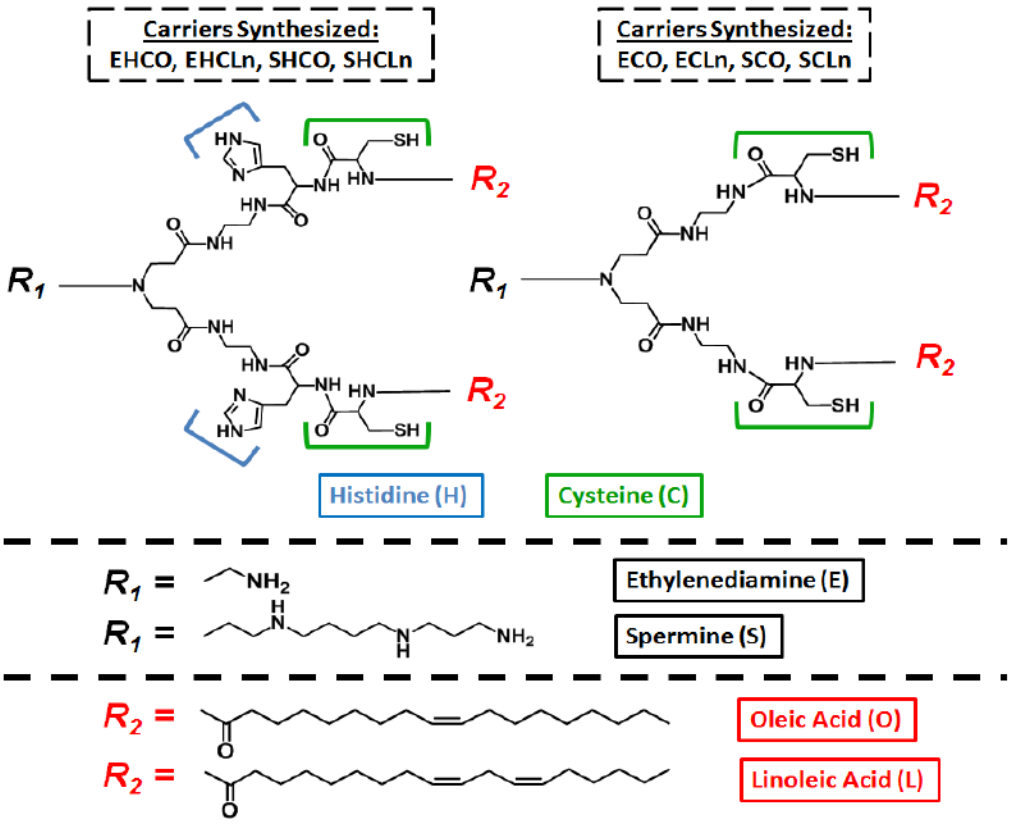

Figure 1.
Chemical structures of the synthesized cationic lipid siRNA carriers

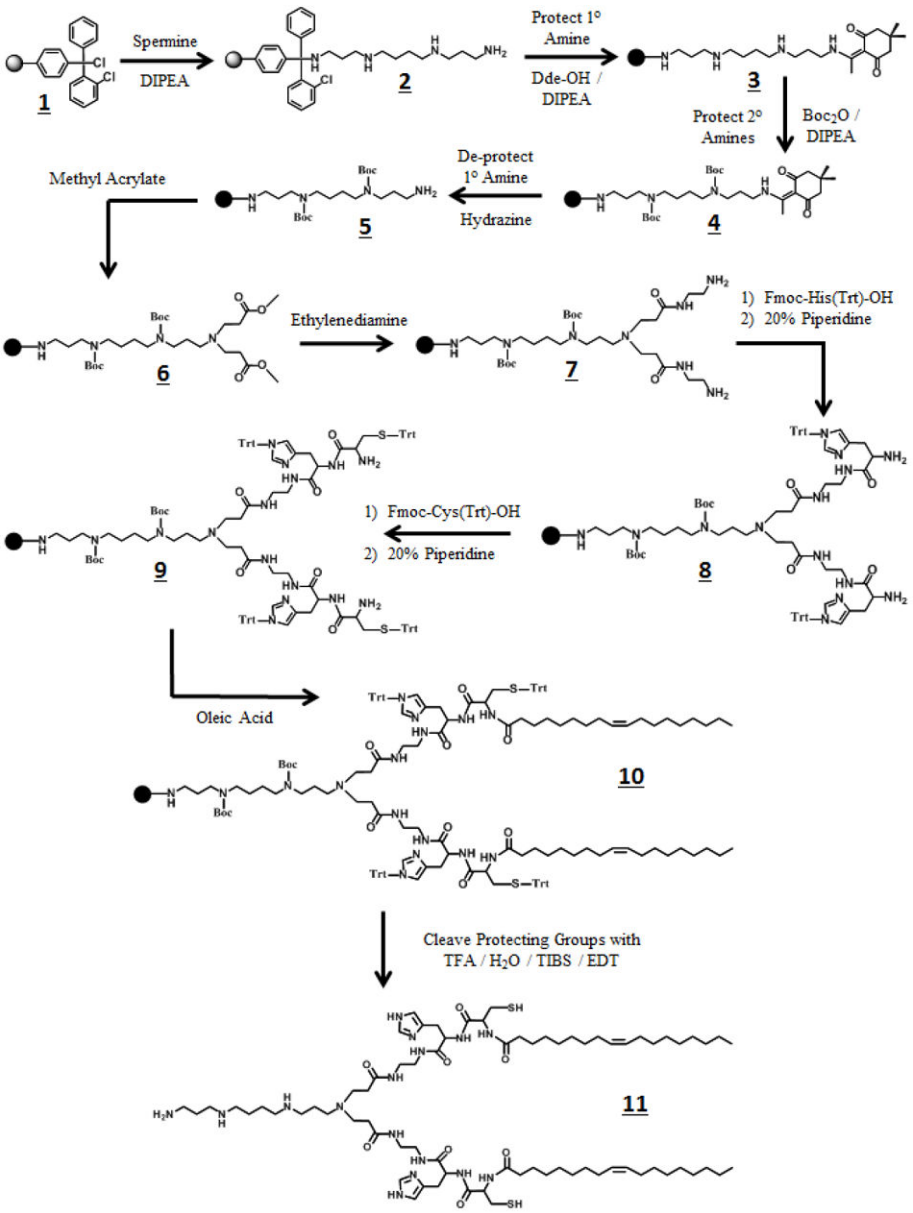

Figure 2.
Reaction Scheme for SHCO

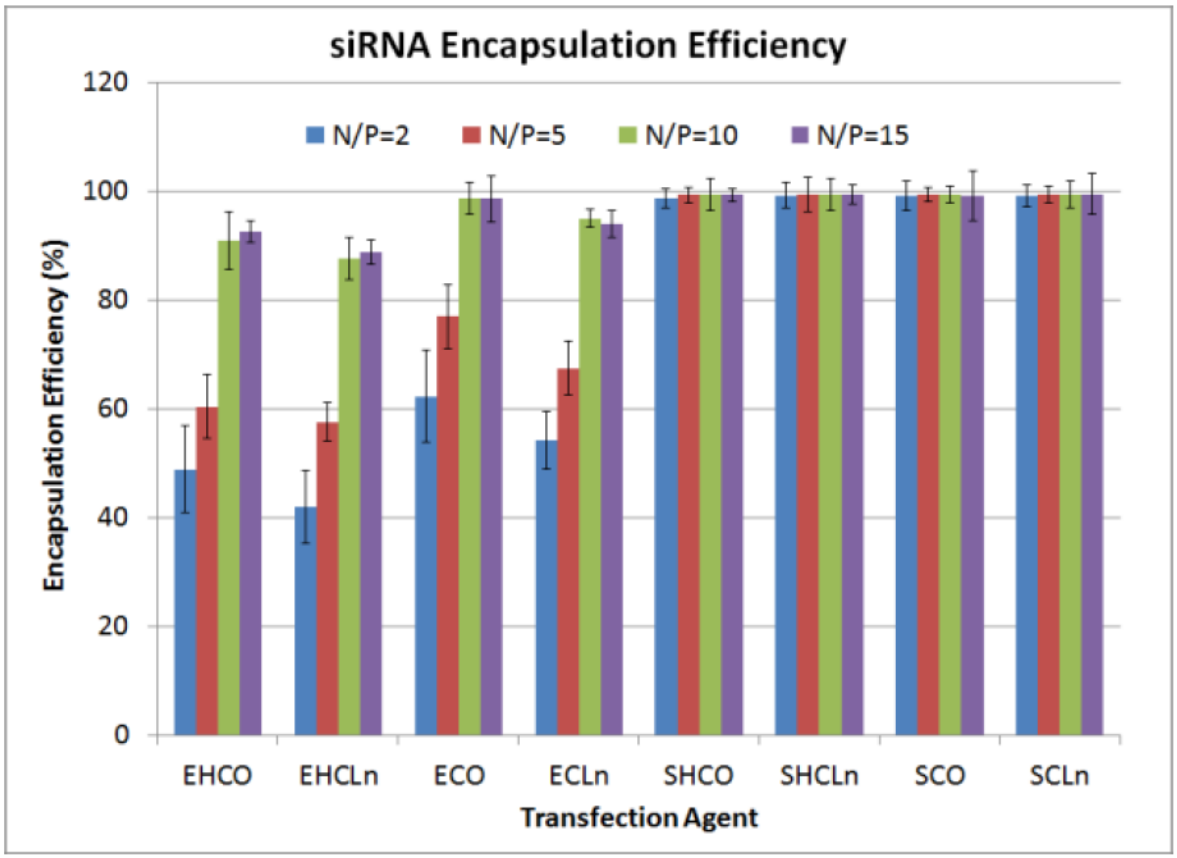

Figure 3.
siRNA encapsulation efficiencies for all carriers in the library over multiple N/P ratios

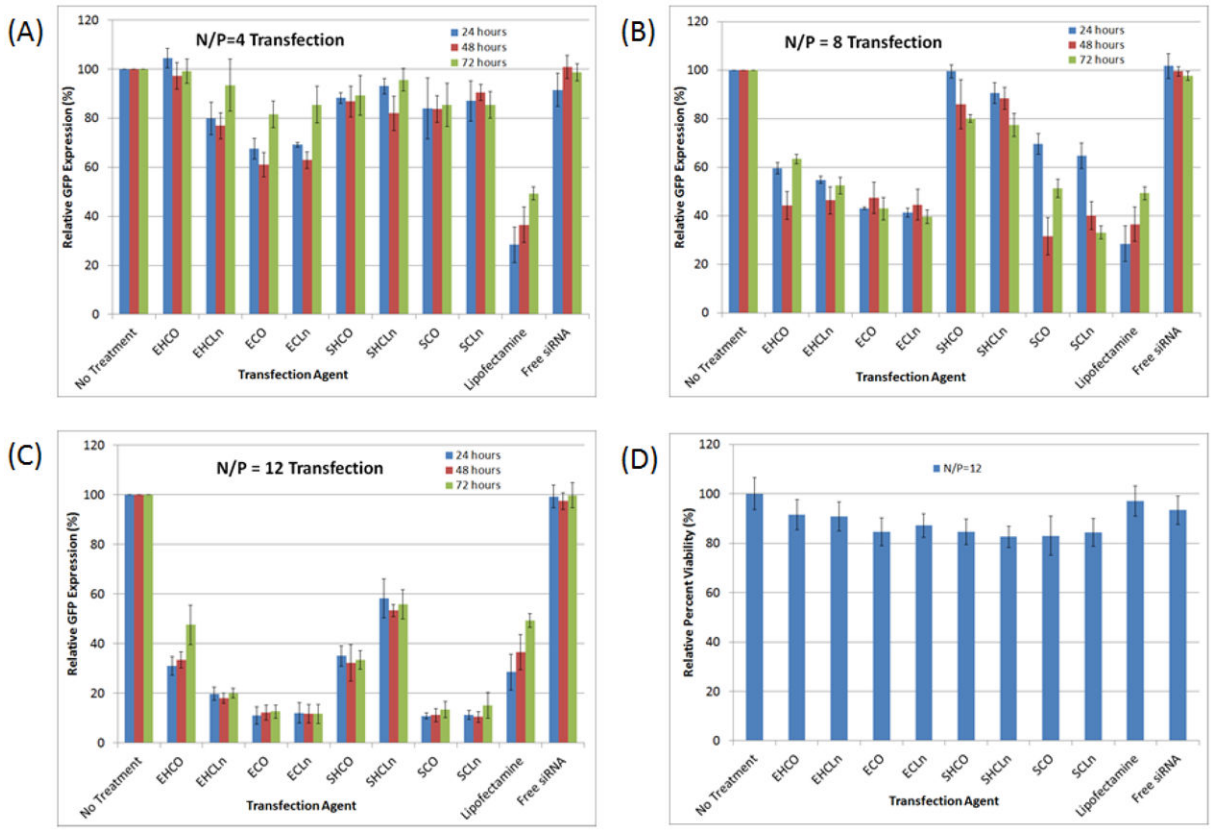

Figure 4.

Silencing of a GFP reporter protein in Chinese Hamster Ovary (CHO) cells was conducted at an siRNA concentration of 100nM over 4 hours, using formulations of N/P=4 (A), N/P=8 (B), and N/P=12 (C). The majority of the carriers were able to reduce GFP expression to at least 20% 72 hours post-transfection. At N/P=12, all but one of the lipid carriers (EHCO) possessed superior long-term silencing capabilities over the commercial agent, Lipofectamine RNAiMax, as evidenced by the fact that GFP expression did not begin to recover at the 72 hour time point. Maximum knockdown of the reporter was achieved at N/P=12 for all the carriers, while maintaining over 80% cell viability (D).

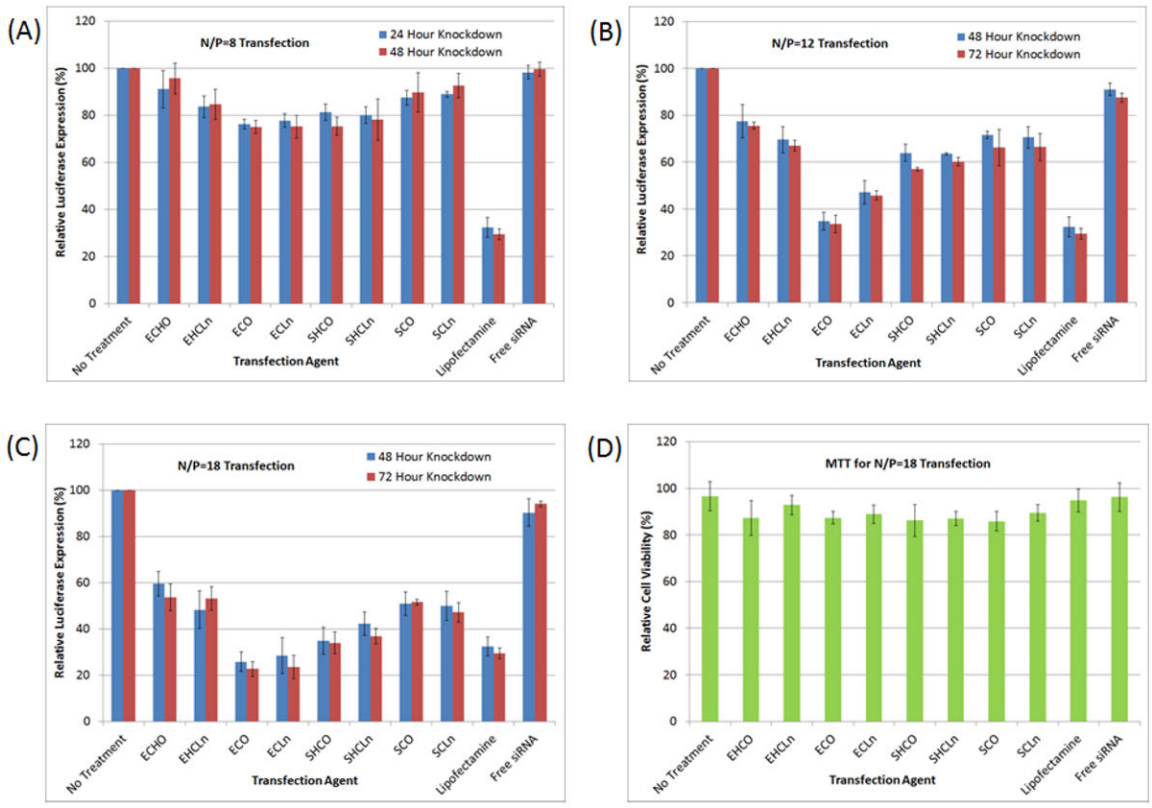

Figure 5.

Silencing of a luciferase reporter protein in HT29 cancer cells was conducted at an siRNA concentration of 100nM over 4 hours, using formulations of N/P=8 (A), N/P=12 (B), and N/P=18 (C). The results above show that ECO and ECL where the most robust of all the carriers 72 hours post-transfection, even out-performing the Lipofectamine RNAiMax commercial agent ($p<0.05$). Maximum knockdown of the reporter was achieved at N/P=18 for all the carriers, while maintaining over 80% cell viability (D).

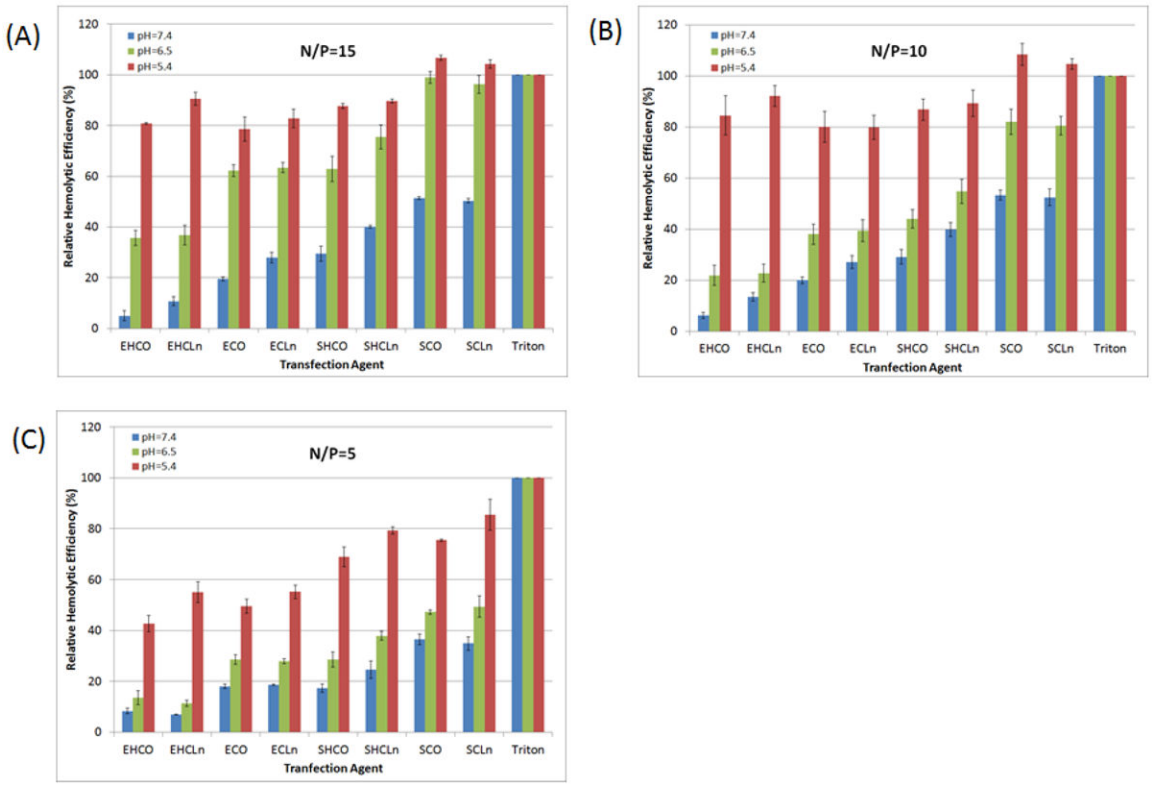

Figure 6.

pH-dependent hemolytic activities of all carriers at N/P lipoplex formulations of 15 (A), 10 (B), and 5 (C). Rat blood cells were diluted 1:50 in PBS and incubated with each formulation at pH=7.4, 6.5, and 5.4 for 2 hours at 37°C. Triton X-100 (1% v/v) was implemented as a positive control. Each carrier exhibited pH-sensitive membrane destabilization properties as the hemolytic activities were found to significantly increase ($p<0.05$) as the acidity of the environment was reduced.

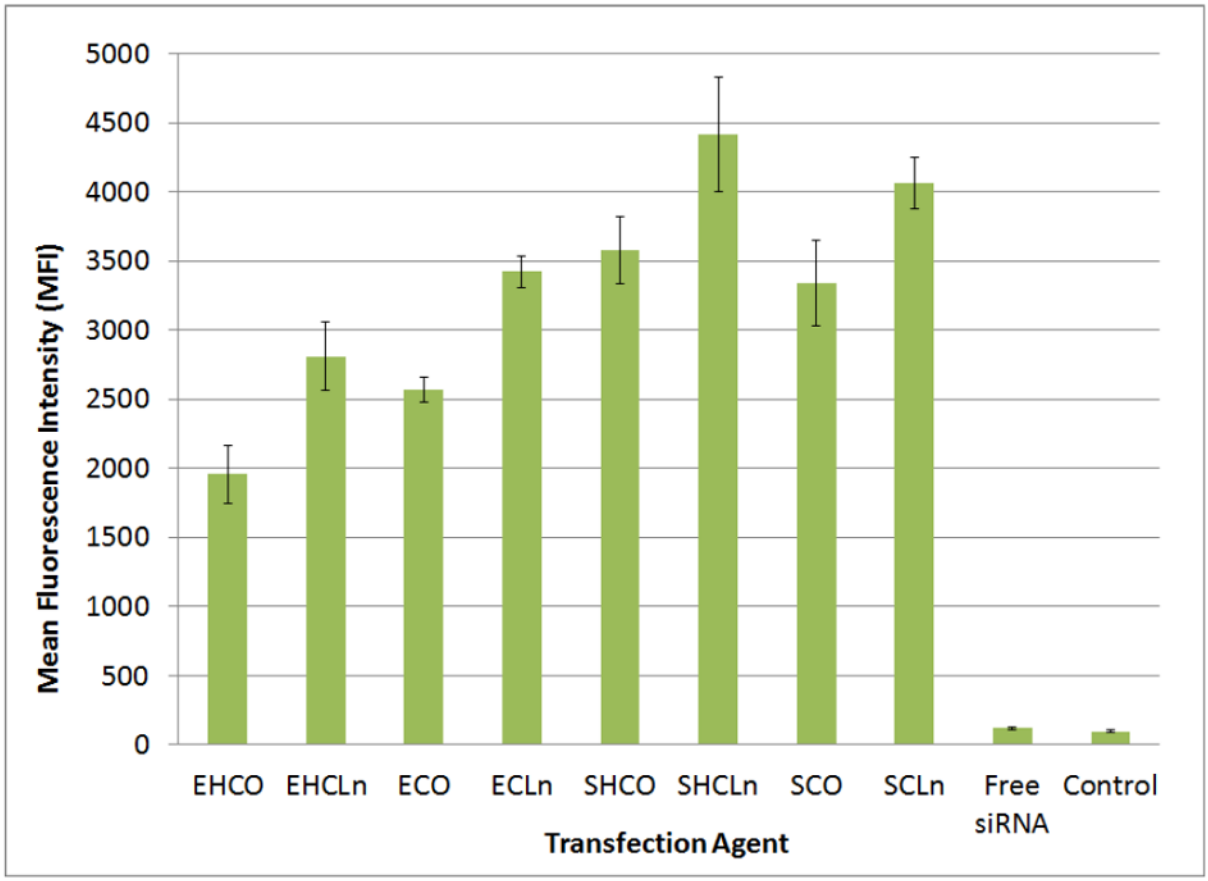

Figure 7.

Flow cytometric analysis of cellular uptake in HT29 cancer cells at N/P=18 formulations. Transfections were performed over a 4 hour period at an siRNA concentration of 100 nM. Mean fluorescence intensity (MFI) values are reported here.

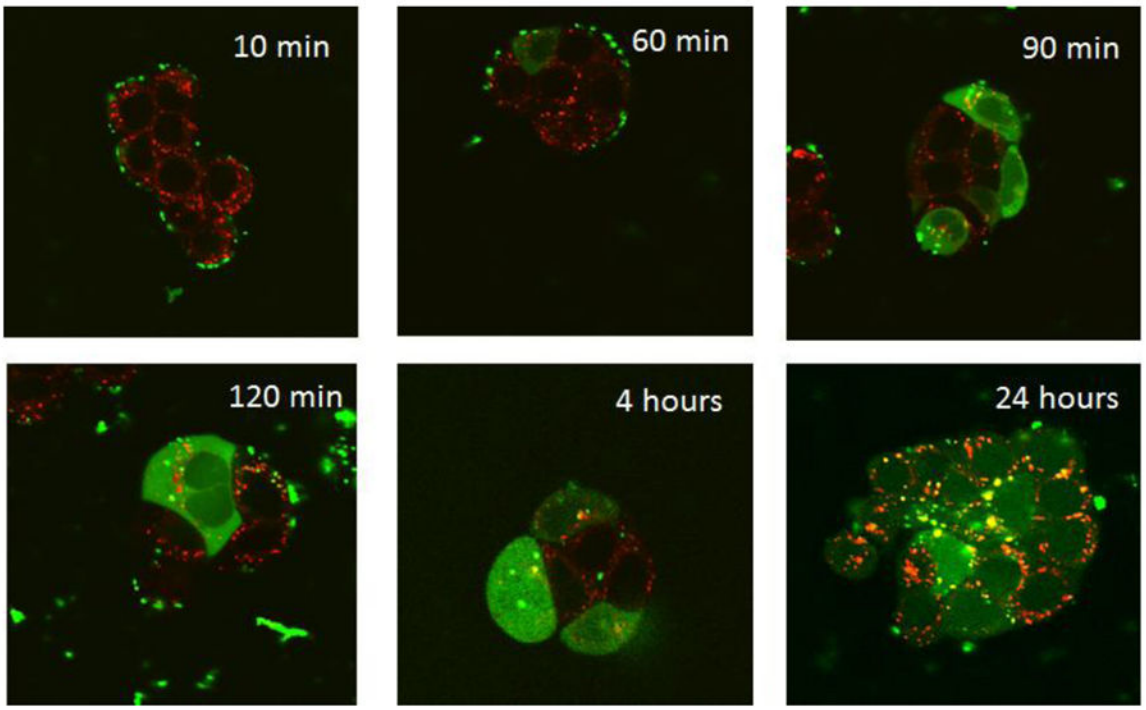

Figure 8.

Confocal imaging shows that the ECO delivery system is able promote intracellular dispersion of siRNA throughout the cytosol (labeled green with Alexafluor-488), preventing degradation within lysosomes (labeled red with Lysotracker Red-DND99). This is evident by the minimal co-localization seen, beginning at the 60 min time point.

Table 1

Measured Mass of Cationic Lipid Carriers by MALDI-TOF Mass Spectrometry

Transfection Agent	Formula	Mw (calc) *m/z*	Mw (found) $[M+1]^+$
EHCO	$C_{66}H_{116}N_{14}O_8S_2$	1296.85	1297.72
EHCLn	$C_{66}H_{112}N_{14}O_8S_2$	1292.82	1293.38
ECO	$C_{54}H_{102}N_8O_6S_2$	1022.74	1023.16
ECLn	$C_{54}H_{98}N_8O_6S_2$	1018.71	1019.11
SHCO	$C_{74}H_{134}N_{16}O_8S_2$	1439.00	1439.86
SHCLn	$C_{74}H_{130}N_{16}O_8S_2$	1434.97	1435.48
SCO	$C_{62}H_{120}N_{10}O_6S_2$	1164.88	1165.42
SCLn	$C_{62}H_{116}N_{10}O_6S_2$	1160.85	1161.19

Table 2

Nanoparticle diameter (nm) as Measured by Dynamic Light Scattering

	EHCO	EHCLn	ECO	ECLn	SHCO	SHCLn	SCOn	SCLn
N/P=2	480 ± 30	403 ± 35	468 ± 43	451 ± 34	441 ± 32	559 ± 38	407 ± 35	482 ± 40
N/P=5	427 ± 25	379 ± 28	448 ± 23	386 ± 20	238 ± 27	233 ± 23	138 ± 28	185 ± 22
N/P=8	380 ± 18	227 ± 20	59 ± 11	126 ± 14	139 ± 17	119 ± 13	63 ± 12	51 ± 14
N/P=10	141 ± 15	130 ± 14	78 ± 12	112 ± 11	151 ± 16	132 ± 15	65 ± 11	50 ± 12
N/P=15	51 ± 10	60 ± 11	42 ± 9	47 ± 12	46 ± 8	75 ± 10	53 ± 9	48 ± 12

Table 3

Polydispersity of siRNA-Lipid Complexes

	EHCO	EHCLn	ECO	ECLn	SHCO	SHCLn	SCOn	SCLn
N/P=2	0.276	0.299	0.245	0.246	0.238	0.246	0.339	0.298
N/P=5	0.195	0.197	0.200	0.276	0.192	0.183	0.236	0.233
N/P=8	0.165	0.167	0.157	0.177	0.189	0.174	0.19	0.140
N/P=10	0.122	0.112	0.136	0.166	0.154	0.114	0.158	0.184
N/P=15	0.161	0.127	0.055	0.120	0.124	0.163	0.176	0.180

Table 4

Zeta-potential (mV) of siRNA-Lipid Complexes at pH=7.4

	EHCO	EHCLn	ECO	ECLn	SHCO	SHCLn	SCOn	SCLn
N/P=2	-23.14 ± 2.47	-23.73 ± 2.26	-32.20 ± 0.90	-26.91 ± 1.37	-32.09 ± 1.65	-31.79 ± 0.94	-29.49 ± 1.33	-28.35 ± 3.61
N/P=5	-14.09 ± 1.88	-17.04 ± 1.32	-16.84 ± 1.58	-18.5 ± 2.43	24.02 ± 1.07	27.40 ± 1.25	26.60 ± 2.76	26.89 ± 1.82
N/P=8	5.54 ± 1.37	0.49 ± 1.17	28.82 ± 1.03	18.32 ± 1.45	26.35 ± 1.40	24.12 ± 4.25	23.16 ± 1.88	26.03 ± 3.66
N/P=10	18.80 ± 1.02	11.34 ± 1.67	25.68 ± 2.02	21.76 ± 2.31	25.59 ± 2.22	26.62 ± 1.47	23.29 ± 3.11	28.59 ± 2.25
N/P=15	22.68 ± 2.08	24.92 ± 2.89	25.19 ± 2.32	23.94 ± 1.70	23.80 ± 2.95	21.91 ± 2.15	25.16 ± 3.75	17.15 ± 2.99